

## Methods for Attaining High Interband Tunneling Current in III-Nitrides

Tyler A. Growden, Sriram Krishnamoorthy, Digbijoy N. Nath, Anisha Ramesh, Siddharth Rajan, and Paul R. Berger

*Department of Electrical and Computer Engineering, The Ohio State University, Columbus, OH 43210, USA*  
*Corresponding author: Tyler Growden, Email: [growden.3@osu.edu](mailto:growden.3@osu.edu), Phone: 614-598-6823*

III-Nitride based tunneling devices have generated a great deal of interest due to their ability to operate at very high powers/current and elevated temperatures. Additionally, with the increasing interest for making GaN-based photovoltaics, the need for efficient interband tunneling in multi-junction solar cells will be a necessity too. But, to date, due to the nitride's large bandgap and lack of very high bulk doping capabilities, it has proved very difficult to create III-Nitride interband tunnel diodes operating at high current densities. One solution is to use a fairly high concentration of indium in the central tunnel junction to decrease the bandgap and thereby exponentially increase the tunneling probability, while also making use of the spontaneous and piezoelectric polarization charge available in the nitrides to supplement the creation of two quantum wells adjacent the tunnel junction, thereby creating a resonant interband tunneling diode (RITD).

Multiple GaN/InGa<sub>N</sub>/GaN RITDs were designed, fabricated, and tested. The device stack shown in Fig. 1(a) displays the growth layer-by-layer, of RITD01. By using an N-polar GaN substrate a very high composition InGa<sub>N</sub> can effectively be grown. Outside of the doped InGa<sub>N</sub> layers, AlGa<sub>N</sub> outside barriers were placed to increase the quantum confinement. On either side of the AlGa<sub>N</sub> barriers, heavily doped caps were placed to promote low-resistance ohmic-like contacts and charge injection. Additionally, Fig. 1(b) shows the device stack for RITD02 which implemented the use of  $\delta$ -doping to exaggerate the band bending effects and sheet carrier concentration induced by the polarization effects at the heterointerfaces.

Tunneling across a narrow junction is highly dependent upon the availability of both carriers and empty energy states on either side of the junction. By increasing the depth of the quantum wells, as well as enhancing the quantum confinement, we can drastically improve the tunneling probability. The band diagrams shown in Fig. 2 are an illustration of RITD01 with and without AlGa<sub>N</sub> outside barriers. Carrier confinement in the conduction band is enhanced by a 0.38 eV additional band offset for the quantum well with the AlGa<sub>N</sub> barrier added, and a 0.09 eV enhancement in QW confinement occurs in the valence band. During forward bias, the QW confined states on either side of the junction will align in energy and interband tunneling will occur. Consequently, deeper quantum wells allow for an increased density of states within the QW, leading to greater tunneling current.

Initial tests showed poor contacts with very low currents and no NDR. But, after cycling the forward sweep multiple times on the same device, the contact essentially self-annealed and a burn-in was achieved, resulting in good ohmic behavior with drastically higher currents. The four sweeps seen in Fig. 3 are immediately following the self-anneal. For each sweep, the PVCR of the NDR decreased drastically, and after the fourth sweep it was nonexistent. Every device tested on this sample exhibited a very similar pattern. Additionally, as has been the case in many nitride-based tunneling diodes, hysteresis was observed. The reverse sweeps shown in the inset of Fig. 3 did not display any NDR, but were very similar in shape and magnitude. The hysteresis in conjunction with the vanishing NDR in the forward sweeps is most likely due to donor-like hole traps found close to the valence band edge near the tunnel junction interface [1]. However, if the reverse sweeps extended beyond a critical voltage, the NDR would reappear in subsequent forward sweeps, suggesting that the traps became depleted. For RITD02 the  $\delta$ -doping created an increase in the depth of the quantum wells, and thus a further increase in the peak tunneling current density was recorded, rising from  $\sim 20$  kA/cm<sup>2</sup> to  $\sim 40$  kA/cm<sup>2</sup>, although there was a drastic decrease in the PVCR. Additionally, the forward sweeps shown in Fig. 4a exhibited a much more stable curve. Finally, Fig. 4b displays that in the reverse there are NDR-like effects, which up to this point has rarely been exhibited in nitride based interband tunneling diodes.

In conclusion, the authors have reported an increase in forward interband tunneling current density from 17.7 A/cm<sup>2</sup> [2] to 39.8 kA/cm<sup>2</sup> by applying outside AlGa<sub>N</sub> confinement barriers and  $\delta$ -doping to a common structure. Some of the devices still exhibit hysteresis effects caused by traps, but some seem to display less of an effect, which needs to be studied further to provide stability. Optimization of the barrier thickness and Indium composition must also be performed to continue to push the peak current density up in value

*Supported by MURI project for III-N Terahertz Electronics, project manager: Paul Maki*

[1] A. Chini, Y. Fu, S. Rajan, J. Speck, , and U.K. Mishra, "An experimental method to identify bulk and surface traps in GaN HEMTs," in *Int. Symp. on Cmpd. Semi. (ISCS)*, 2005. [2] S. Krishnamoorthy, P.S. Park, S. Rajan, "Demonstration of forward inter-band tunneling in GaN by polarization engineering," *Appl. Phys. Lett.*, vol. 99, no. 23, Dec. 2011.

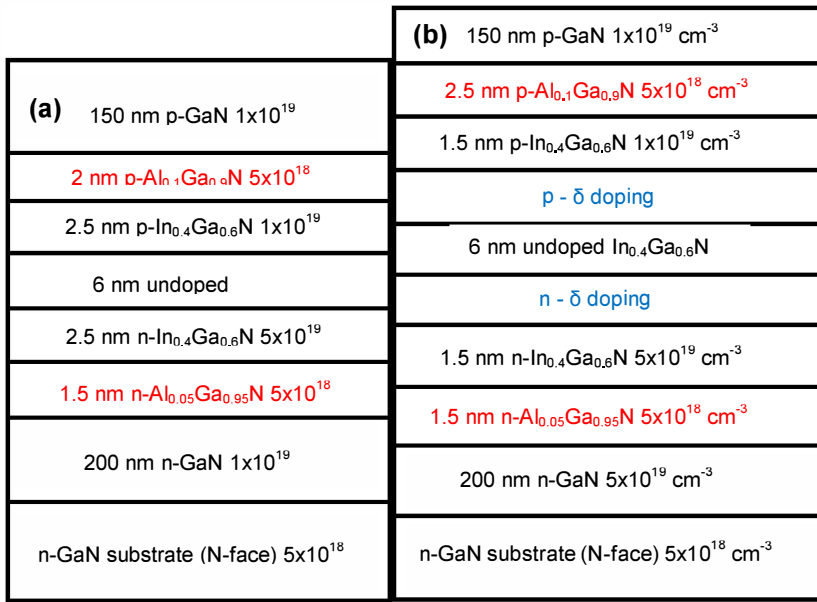


Figure 1: (a) Schematic of RITD01 with outside AlGaIn barriers. (b) Schematic of RITD02 with outside AlGaIn barriers as well as delta doping layers.

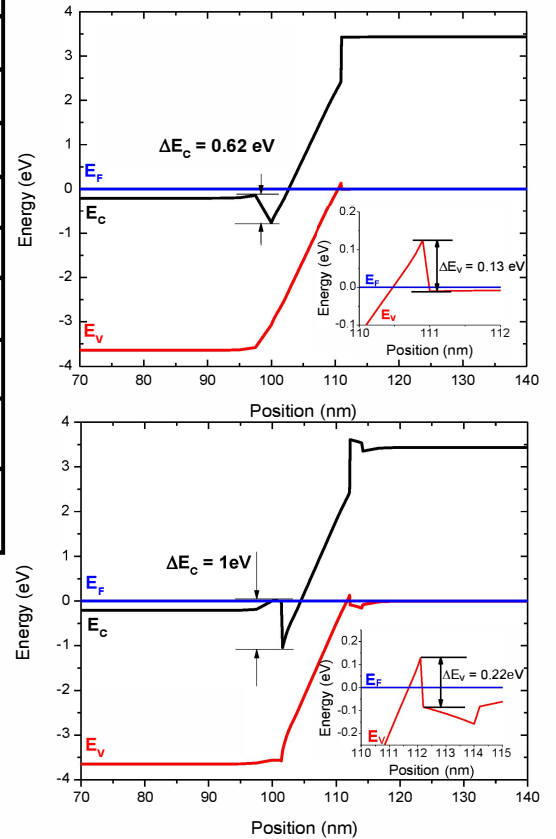


Figure 2: (a) The calculated band diagram of a device without AlGaIn outside barriers. (b) The calculated band diagram of RITD01 with AlGaIn outside barriers included. The conduction band and valence band (inset) QW offsets are illustrated for clarity.

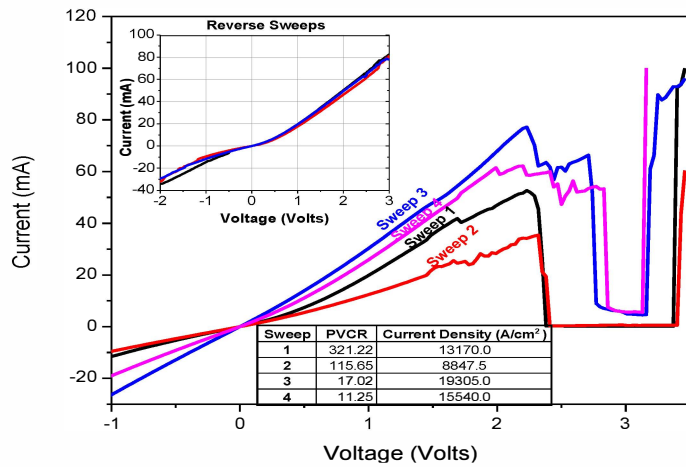


Figure 3: The IV curves for 4 subsequent tests located on RITD01. The top left inset shows 3 reverse sweeps on the same device. The bottom inset displays the relative PVCRs and current densities.

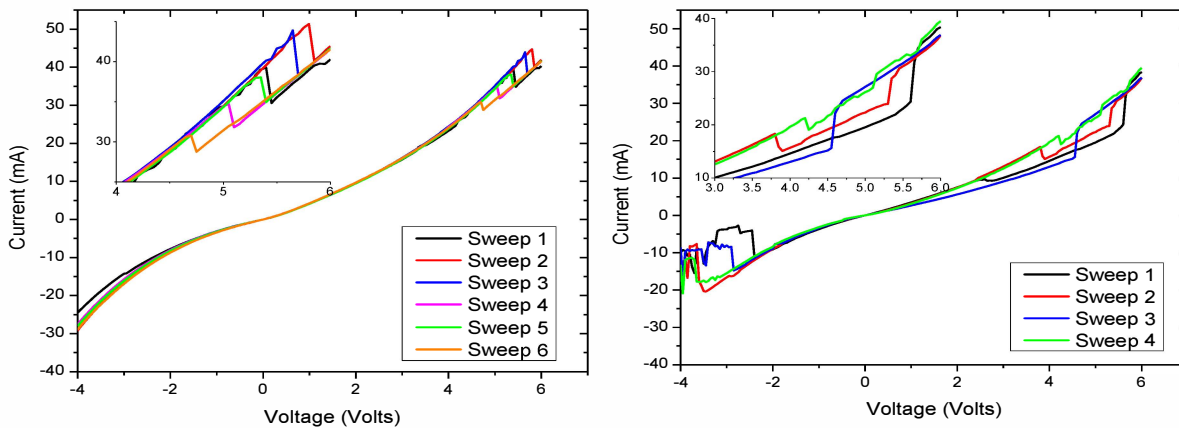


Figure 4: (a) The forward sweep IV curves for RITD02. (b) The reverse sweep IV curves for RITD02, which are displaying NDR-like behavior.